PCCP

Accepted Manuscript

ROYAL SOCIETY OF CHEMISTRY

www.rsc.org/pccp

Ab-initio calculations on $^1O_2$ quenching mechanism by *trans*-resveratrol

Gloria Mazzone,* Marta E. Alberto, Nino Russo and Emilia Sicilia

Dipartimento di Chimica e Tecnologie Chimiche, Università della Calabria, I-87036 Arcavacata di Rende (CS), Italy

*To whom correspondence should be addressed

Fax. +39-0984-492044, Tel. +39-0984-493342

e-mail: gloria.mazzone@unical.it

Abstract

Trans-resveratrol showed to play an important role in a variety of biological and medical processes such as reactive oxygen species (ROS) scavenging, inhibition of apoptosis and induction of cell survival. In light of the fact that resveratrol and its oligomers were found to be selective singlet oxygen $^1O_2$ quenchers, we report here a systematic study on the reactivity of *trans*-resveratrol toward molecular oxygen in acetone simulated media. On the basis of the controversial hypotheses reported in literature we explored, at density functional level of theory, two different mechanisms. The first one leads to resveratrol quinone product via an endoperoxide intermediate by attack of $^1O_2$ on the resorcinol ring, assisted (pathway (b)) or not (pathway (a)) by a water molecule. The second mechanism, in which the singlet oxygen reacts with the double bond connecting the two resveratrol rings leading to benzaldehyde products, involves the formation of a dioxetane intermediate. As the outcomes of our computational analysis show that the latter mechanism is kinetically more favorable than the former one, it is likely that when *trans*-resveratrol reacts with singlet oxygen a dioxetane intermediate is formed.

Keywords: trans-resveratrol, quenching mechanism, ROS, singlet molecular oxygen, DFT

Introduction

Resveratrol (3,5,4'-trihydroxystilbene) is a naturally occurring phytoalexin which is synthesized by plants in response to adverse conditions, such as environmental stress or pathogenic attacks.[1] Resveratrol exists as *trans* and *cis* isomers, both found in wines and other plant fruits with different concentrations depending on weather conditions.[2] The two isomers seem to behave in similar manner, but the *cis* is surely less active than the *trans* isomer.[3]

In recent years, resveratrol, especially the *trans* isomer, has attracted much interest in the field of diseases prevention and slowing aging.[4] Early published papers suggest that it exerts its biological activity against various diseases through a variety of processes, whose underlying mechanisms are still poorly understood,[5] such as reactive oxygen species (ROS) scavenging, inhibition of apoptosis or induction of cell survival. Among such properties, scavenging of reactive oxygen species (ROS) are of special interest in medicine and biological chemistry due to the strong evidence that ROS are implicated in the pathogenesis of many degenerative diseases, like Parkinson's, autoimmune, multiple sclerosis diseases, and aging in humans.[6] The known forms of ROS include oxygen radicals, like the superoxide radical anion (O_2•−), hydroxyl radical (•OH), alkoxyl (•OR) and peroxyl (•OOR) radicals, but also non-radical oxidizing agents such as ozone (O_3), hydrogen peroxide (H_2O_2), hypochlorous acid (HOCl) and singlet oxygen ($^1O_2$).[7]

In a previous work[8] one of us performed a systematic quantum-chemical study on the reactivity of trans-resveratrol towards the hydroxyl (•OH) and hydroperoxyl (•OOH) radicals in aqueous media. The main conclusion of mechanistic and kinetics calculations is that, since the •OOH half-life time is several orders larger than that of the •OH radical, trans-resveratrol acts more efficiently as •OOH (and probably other structurally similar •OOR radicals) than •OH scavenger, following the only thermodynamically feasible reaction channel in water, that is a hydrogen atom transfer (HAT) mechanism by H-abstractions from the phenolic groups.[8]

In this work, we have focused our attention on the reactivity of singlet oxygen ($^1O_2$), the first excited state $^1\Delta_g$ of molecular oxygen, toward resveratrol. $^1O_2$ is one of the most active species

involved in chemical and biochemical reactions, since it can react with a huge variety of biological molecules, containing carbon-carbon double bond such as DNA, proteins and lipids.[9]

Production of the metastable singlet oxygen state in biological systems is achieved by phagocytosis of neutrophils,[10] photosensitized oxidations[11] or bimolecular decomposition of lipid hydroperoxides.[12] Most of the research on the singlet oxygen oxidation was carried out exploring two different aspects of this topic: the singlet oxygen formation and its role in the production of specific compounds and the study of the quenching mechanisms and kinetics of quenchers.

A good quencher is a molecule able to rapidly interact with singlet oxygen, deactivating its excited state. Deactivation can be accomplished by either physical or chemical quenching. Physical quenching leads only to the deactivation of singlet oxygen to its ground state with no oxygen consumption or product formation. In chemical quenching, instead, singlet oxygen reacts with the quencher to form oxidation products. In biological systems, $^1O_2$ is involved in reactions with organic molecules and different products can be obtained. For instance, the reaction of O_2 ($^1\Delta_g$) with olefinic and aromatic double bonds leads to hydroperoxides and endoperoxides, respectively. Examples of molecules that are commonly used as quenchers include azide anion,[13] 1,4-diazabicyclo[2.2.2]octane (DABCO), histidine and various carotenoids, such as ß-carotene.[14]

Recently, resveratrol and its oligomers from wine grapes were found to be selective singlet oxygen $^1O_2$ quencers.[15] On the basis of HR-FTICR-MS experiments and PM3 semiempirical calculations, the authors assert that, similarly to other phenolic species, the reaction of resveratrol with $^1O_2$ leads to the formation of quinones, via an endoperoxide intermediate (as depicted in Scheme 1). As suggested by the authors, the first step of the title reaction is 1,4-cycloaddition of $^1O_2$ to the resorcinol ring of resveratrol, forming the endoperoxide intermediate. From here, the reaction can proceed following two different ways: the first pathway involves an intramolecular H-abstraction (pathway (a)) to generate the resveratrol quinone, through the formation of an hydroperoxide intermediate, in which the carbonyl C=O is already formed; the second one (pathway (b)) is an hydrolysis process to form an unstable hydroperoxide intermediate with

consecutive loss of a water molecule, that evolves to the same hydroperoxide intermediate involved in the first path.

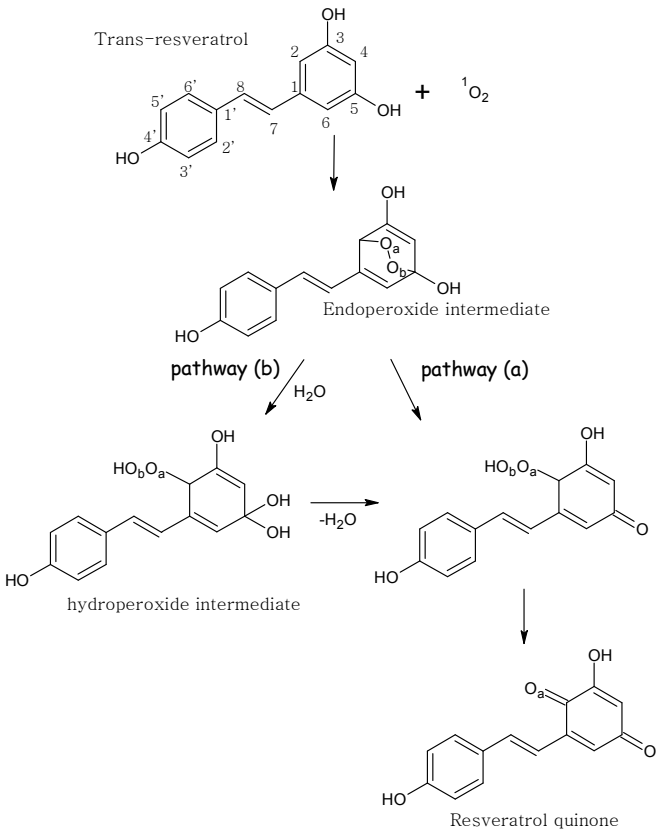

Scheme 1

The reaction mechanism was hypothesized on the basis of HPLC-ESI-MS^2 results, which led the authors to assert that resveratrol quinones are the main products of the reaction between resveratrol and $^1O_2$. Since in the MS^2 spectra the peak for the neutral loss of C_2H_2O, characteristic of the resorcinol ring in resveratrol,[16] was not found the authors suppose that resorcinol ring is converted to quinones during the quenching. Furthermore, as a peak attributable to 4-hydroxybenzaldehyde was found, it is hypothesized that it is generated by resveratrol photolysis. Since benzaldehyde molecular weight is much lower than that of resveratrol quinones, the possibility that it could be the product of the oxidation process was not taken into account.

A very recent combined theoretical and experimental work, carried out to shed light on the photochemical oxidation of resveratrol, showed how benzaldehydes should be the only product of the reaction between *cis*-resveratrol and $^1O_2$.[17] On the basis of the exploration of two different dehydrogenation pathways, the authors conclude that the formal [π2+π2] cycloaddition reaction, which leads to benzaldehydes via a dioxetane intermediate, is the favored pathway from both kinetic and thermodynamic points of view. For that reason, we have also considered the possibility that *trans*-resveratrol, similarly to the *cis* isomer, can undergo the attack of singlet molecular oxygen on the exocyclic double bond, following the [π2 +π2] cycloaddition pathway, according to the mechanism depicted in Scheme 2.

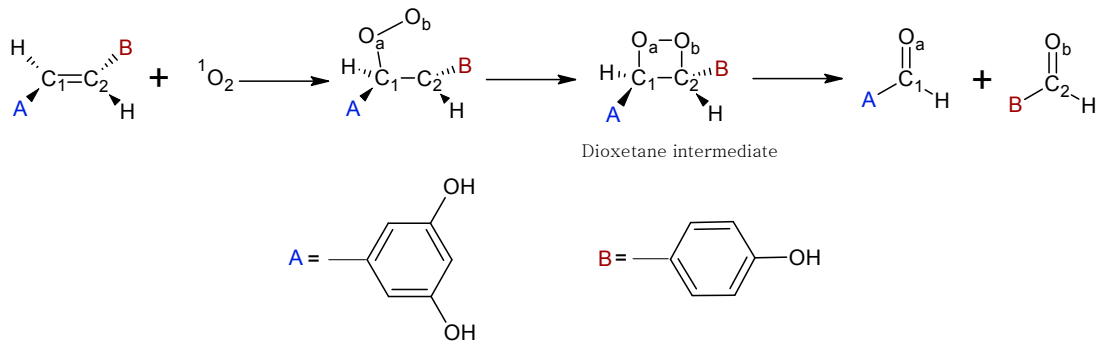

Scheme 2

As the investigation and understanding of the mechanism of antioxidative action of resveratrol and its derivatives can provide basis for designing compounds with better antioxidant activities, *trans*-resveratrol was selected as a model molecule to investigate its behavior towards $^1\Delta_g$ molecular oxygen. With the aim to supply a more detailed description of the quenching mechanism than that previously obtained by performing very undemanding semiempirical calculations,[15] we carried out a systematic exploration of all the proposed mechanisms by means of both density functional theory (DFT) and Möller-Plesset perturbation theory (MP2).

Computational Details

All molecular geometries have been fully optimized in solvent at the DFT level of theory, using both the Becke3-LYP (B3LYP)[18,19], one of the most widely used hybrid density functionals, and the more recently developed M052X[20] in conjunction with the 6-31G** standard basis set. The M052X exchange correlation functional was recently proven to give both reliable results in reaction involving radical species and accurate description of loose-type interactions.[20,21]

The impact of solvent effects on the calculations carried out by using the B3LYP functional, was taken into account by using the Conductor Polarizable Continuum Model (CPCM)[22] in conjugation with the UFF set of radii to build-up the cavity. The SMD continuum model,[23] instead, was selected for solvent effects refined calculations executed employing M052X as exchange correlation functional, according to suggestions reported in literature.[20] The surrounding acetone medium was characterized by its dielectric constant ε=20.

Local minima and transition states were identified by harmonic vibrational frequencies calculations: real frequencies for local minima and a single imaginary frequency, which corresponds to the expected motion along the reaction coordinate, for transition states. All the intercepted transition states were checked by IRC (intrinsic reaction coordinate) analysis.[24] For all the intercepted minima and transition states, the stability of the wave function has been checked.

Single-point calculations on the optimized geometries of minima and transition states at the same level of theory were carried out employing the large 6-311++G(3df,2p) standard basis sets for all the atoms to calculate final energies.

The optimized structures of stationary points were also used to perform single-point calculations by using second-order Möller-Plesset perturbation theory (MP2), within the approximation resolution of identity (RI-MP2)[25] as implemented in Turbomole Package (version 6.3),[26] along with the split-valence basis set SVP for all the atoms. To improve the accuracy of the correlation energies calculated in the framework of second-order Møller–Plesset perturbation theory, the spin-component scaling (SCS) approach was used.[27]

$\langle S^2 \rangle$ values for all the optimized structures were checked to assess whether spin contamination can influence the quality of the results. In some cases unrestricted calculations revealed triplet spin contamination, since $\langle S^2 \rangle$ values close to 1.0 were found. In such cases, the method proposed by Ovchinnikov and Labanowski was adopted for correcting the mixed spin energies and removing the foreign spin component. [28] For instance, the unrestricted calculation of the singlet energy of O_2 gave a $^1\Delta_g$ state too much stable due to the contamination of the singlet wave function with the triplet state. The corresponding excitation energy of 10.4 kcal/mol was calculated, being the experimental value 22.5 kcal/mol. By using the singlet state corrected energy a triplet–singlet energy gap of 21.0 kcal/mol was obtained, in very good agreement with the experimental value.

Results and Discussion

In the next sections are illustrated the outcomes of the computational exploration of the reactivity of *trans*-resveratrol toward $^1\Delta_g$ singlet molecular oxygen with the support of the information coming from experiments. Since weak interactions play an important role in the initial steps of the explored mechanisms, here only the results of the analysis performed employing the M052X functional are illustrated, while both B3LYP and SCSRIMP2 results are reported in the Supporting Information.

1,4-cycloaddition pathway: formation of quinones via endoperoxide intermediate

As a first step of the work we explored the 1,4-cycloaddition pathway and the computed M052X free energy profile is reported in Figure 1. Fully M052X optimized structures of stationary points intercepted along both the (a) and (b) investigated pathways, are shown in Figure 2, in which some selected geometrical parameters are included.

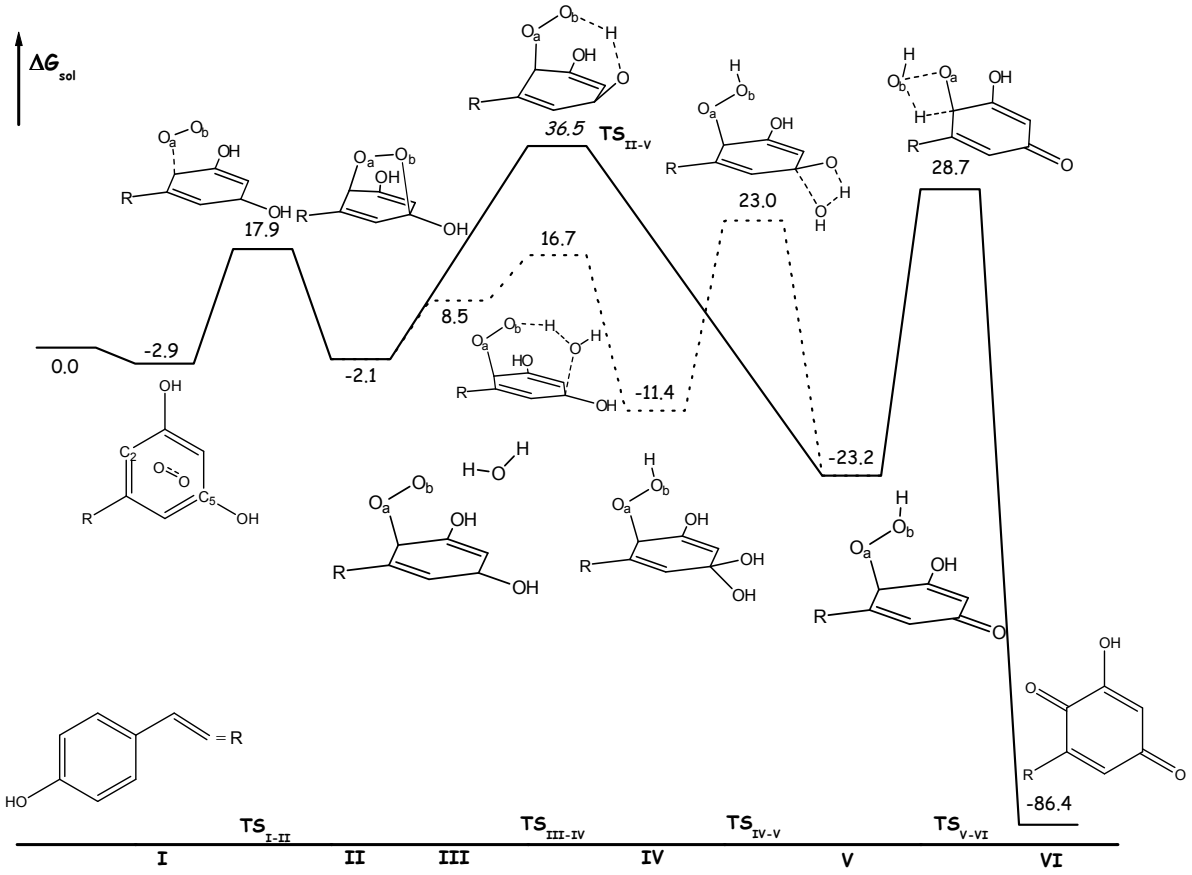

Figure 1. M052X free energy (kcal/mol) profile for the 1,4-cycloaddition mechanism. The solid and dotted lines describe the (a) and (b) pathways, respectively.

The resveratrol molecule contains both resorcinol and phenol moieties. Because of the conjugated double bond connecting them, resveratrol has a planar structure, with a torsion angle of 179.9°. Looking at both Figures 1 and 2, it is evident that the first step along the 1,4-cycloaddition pathway for the quenching mechanism of $^1O_2$ by *trans*-resveratrol involves a preliminary interaction between reactants, which leads to the formation of an adduct labeled **I**, where the molecular oxygen weakly interacts with the resorcinol ring. Two covalent bonds, instead, are formed by the two oxygen atoms with the C2 and C5 atoms (see Scheme 1) of the resorcinol ring in the adduct **II**. The approach of molecular oxygen to *trans*-resveratrol is examined by comparing frontier molecular orbitals plots (Figure 3) for both **I** and **II** adducts. As can be seen from the HOMO plot, while in the first species the singlet molecular oxygen interacts with the whole π system of resveratrol, in the second one, in which O_a and O_b atoms are directly bound to the C2 and C5 atoms of the resorcinol

ring, respectively. The established interaction entails the loss of the ring aromatic character and the overlapping of the orbitals of the covalently bonded C and O atoms is shown in the plot of the molecular orbital in Figure 3.

In the adduct **I** there is no direct interaction between the oxygen atoms of the O_2 molecule and the resveratrol molecule. The two oxygen atoms lie at 2.600 and 2.698 Å from the C2 and C5 atoms, respectively and, as a consequence, the planarity of *trans*-resveratrol is not affected (see Figure 2).

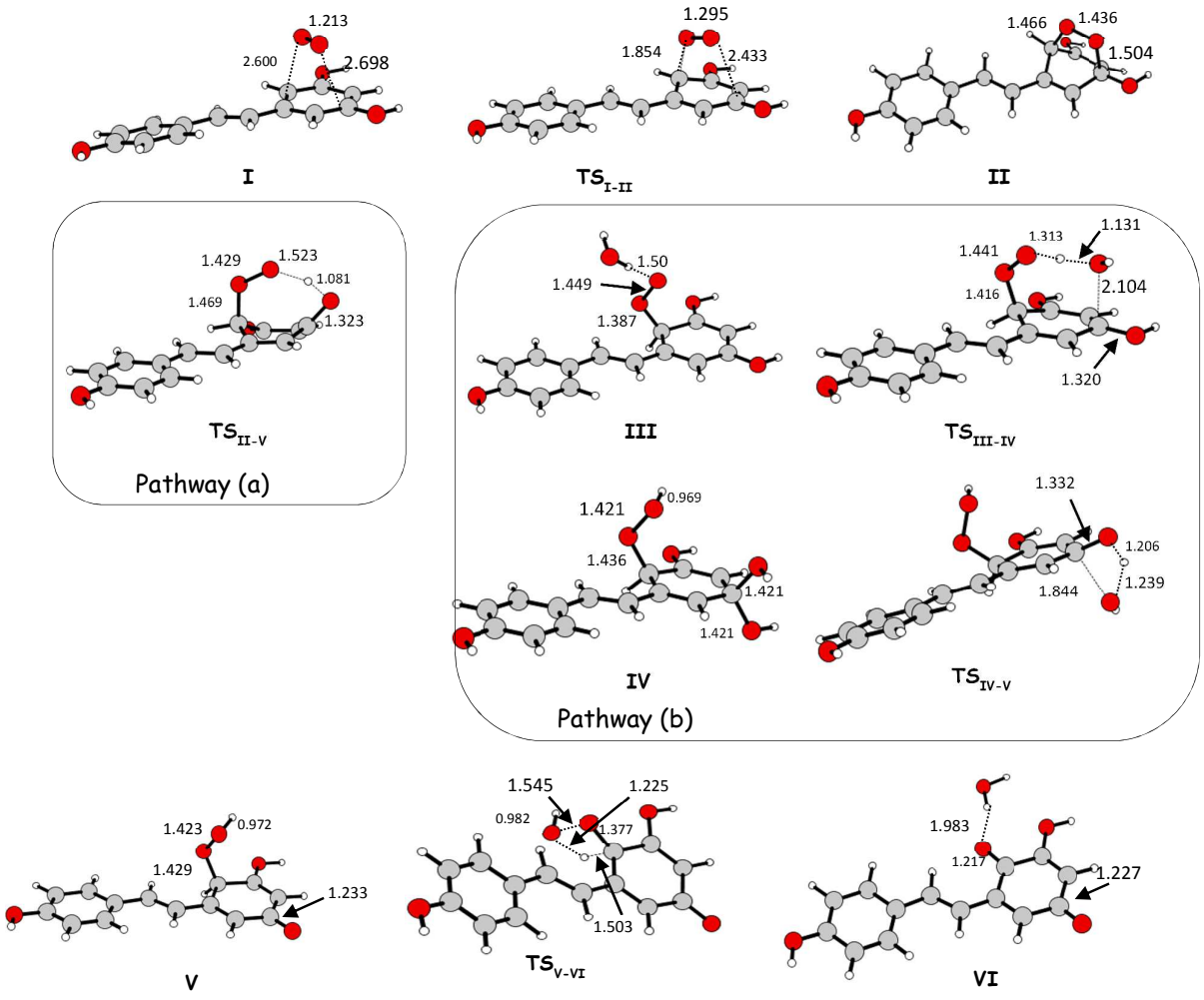

Figure 2. Optimized structures of all the intermediates and transition states intercepted along the 1,4-cycloaddition pathway. Bond lengths are in Å.

In the adduct **II**, instead, the formed covalent bonds, C2-O_a (1.466 Å) and C5-O_b (1.504 Å), cause a planarity distortion of the ring and both C2 and C5 atoms temporarily slightly change their hybridization. This conclusion can be drawn also looking at the O-O distance, which from 1.215 Å in the $^1O_2$ isolated molecule becomes 1.436 Å in the intermediate **II**. In the preliminary adduct **I**, instead, the O-O distance (1.218 Å) is almost the same than that of the isolated $^1O_2$ molecule, confirming a weak interaction between such molecule and the π-system of the resorcinol ring.

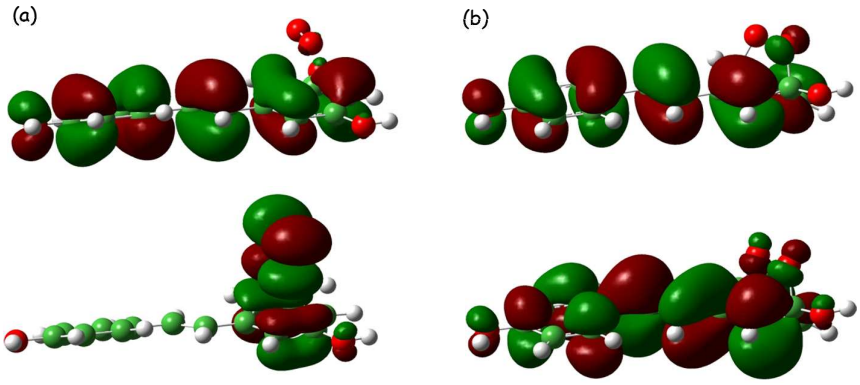

Figure 3. HOMO (on top) and LUMO (on bottom) plots of (a) **I** and (b) **II** adducts, respectively.

The **I** adduct lies 2.9 kcal/mol lower in energy with respect to the reference energy, that is the sum of reactants' energies. The adduct **II**, is then formed overcoming an energy barrier of 20.8 kcal/mol (through the $\mathbf{TS_{I\text{-}II}}$). In the transition state $\mathbf{TS_{I\text{-}II}}$ the O_a atom approaches the C2 one at a distance of 1.854 Å and with an angle O_b-O_a-C2 of 112.9°, while the O2 atom lies at 2.433 from the C5 one. In the transition state it is already evident the partial loss of aromatic character of the resorcinol ring, because of its planarity distortion. In the intermediate **II**, which is slightly less stable than the previous one the ring assumes a like-boat conformation, with C2 and C5 atoms coming out of the ring plane.

It is worth noting some significant differences between M052X and B3LYP outcomes concerning the first reaction step as described above. Since the M052X functional allows a better description than the B3LYP one of the initial non-covalent interaction between reactants a different

stabilization of **I** adduct is calculated. Indeed, **I** adduct is more stable by 2.9 kcal/mol than the separated reactants at the M052X level, while the B3LYP optimization results in a destabilization of 5.5 kcal/mol with respect to the reference energy (Figure S3). Since the next transition state $\mathbf{TS_{I\text{-}II}}$ lies at the same energy for both functionals, as a consequence, the energy required to form the adduct **II** is higher along the M052X pathway than for the B3LYP one (20.8 vs 12.4 kcal/mol). Furthermore, a significant structural difference can be underscored. Though the C-O bonds formation causes the loss of the ring aromatic character in both cases, the ring assumes a like-boat conformation when the M052X functional is employed, while at the B3LYP level only a slightly distortion of the ring planarity occurs (see Figure S3).

Once formed the adduct **II**, the reaction can proceed following two different pathways. The first one, pathway (a), involves an intramolecular H-abstraction to generate resveratrol quinones, through the formation of a hydroperoxide intermediate. We intercepted a transition state, $\mathbf{TS_{II\text{-}V}}$, with an activation energy barrier of 38.6 kcal/mol, in which the H atom moves away from the 5O atom in order to form the hydroperoxide group in intermediate **V**. In the optimized structure, the O2-C5 bond is already broken, the O_a-O2 distance becames 1.429 Å and the incoming H atom lies at 1.523 Å from O2 one. The hydroperoxide intermediate **V** is, thus, generated with an energy gain of 23.2 kcal/mol. In such intermediate the C2-O_a bond is stronger than in the species **II** (1.429 Å vs 1.466 Å), while the distance between the O_a and O_b atoms becomes 1.423 Å. The subsequent step is the release of a water molecule from the hydroperoxide intermediate **V**, which is realized, through the $\mathbf{TS_{V\text{-}VI}}$, overcoming an energy barrier of 51.9 kcal/mol. In the $\mathbf{TS_{V\text{-}VI}}$, the H-abstraction from the C2 atom to form the water molecule causes the definitive breaking of the O_a-O_b bond, which becomes 1.545 Å, while the O_b atom approaches the H one at a distance of 1.225 Å. In the formed resveratrol quinone **VI** the established chetonic functionality strongly stabilizes the final product, which lies 86.4 kcal/mol lower in energy than the separated reactants.

The intermediate **V** can be obtained following a different pathway, named pathway (b), in which a water molecule assists the formation of such hydroperoxide, which is now achieved in two

steps. The first step of this path involves a preliminary interaction between the intermediate **II** and the water molecule which is realized in the adduct **III**, whose formation requires 10.6 kcal/mol to occur. In the intermediate **III** a water proton interacts with the O_b atom (at a distance of 1.506 Å) causing an elongation of the O_a-O_b bond and a shortening and O_a-C2 one, with respect to the adduct **II**. The O_a-O_b distance, starting from 1.436 Å becomes 1.449 Å in the adduct **III**, while the O_a-C2 distance decreases from 1.466 Å to 1.387 Å. The formation of the hydroperoxide **IV** is realized through the transition state $\mathbf{TS_{III\text{-}IV}}$, in which the attack of the water molecule oxygen on the C5 atom occurs concomitantly with the transfer of its proton to the O_b atom. Thus, the O_b-H bond is almost already formed, since H atom lies at 1.131 Å and 1.313 Å from the water oxygen atom and the O_b atom, respectively. Formation of the adduct **IV**, which lies 19.9 kcal/mol below the adduct **III**, is accomplished overcoming an energy barrier of 8.2 kcal/mol. In the second step, a water molecule is released from the intermediate **IV** as a result of an intramolecular H atom shift from one of the two OH groups bound to the C5 atom in favor to the other one in order to establish the ketonic functionality. In the involved transition state, $\mathbf{TS_{IV\text{-}V}}$, the C5-O bond, which in the adduct **IV** was 1.421 Å, is elongated to 1.844 Å as well as the O-H bond of the hydroxyl group that remains bound to the C5 atom. Thus, the adduct **IV** is transformed to the hydroperoxide intermediate **V**, overcoming an energy barrier of 34.4 kcal/mol. Once formed the intermediate **V**, the reaction proceeds to form the final product as already described above.

The final release of the water molecule, occurring indifferently if the reaction follows the pathway (a) or (b), is the step that controls the reaction rate, since it requires the overcoming of the highest energy barrier (51.9 kcal/mol). In the stepwise mechanism (b) the first and second steps require 8.2 kcal/mol and 34.4 kcal/mol, respectively, to take place. Following the pathway (a) an amount of energy equal to 38.6 kcal/mol is required for the formation of the hydroperoxide intermediate **V**. It is worth noting that formation of such hydroperoxide intermediate does not correspond to the rate limiting step of the whole process. On the contrary, the outcomes of PM3 semiempirical molecular orbital calculations suggest the pathway (b) as the most probable one

because the barrier along the pathway named (a) is higher than the barriers along the pathway (b).[15] Moreover, the first step along pathway (b) is indicated as the rate determining step of the whole process.

With the aim to establish whether it is possible to clearly indicate which of the two pathways is the preferred one, additional calculations were performed, employing a different exchange-correlation functional, such as B3LYP, and a different level of theory, namely MP2.

For an easier comparison the energy barriers, computed at different levels of theory for the steps involved in both (a) and (b) pathways and that we calculated to be the rate determining step, are collected in Table 1.

As reported in figure S1 of the supporting information and in Table 1, calculations carried out employing a different functional, indicate the final step for the formation of the resveratrol quinone product as the step that controls the reaction rate. The height of the energy barriers computed for the only step of pathway (a) and for the second step of pathway (b) (34.4 and 27.6 kcal/mol, respectively) is comparable.

Table 1. Free energy barriers in solution (ΔG_{sol}, in kcal/mol) calculated at different levels of theory for all the steps along the investigated energy profiles.

	TS_{II-V}	TS_{III-IV}	TS_{IV-V}	TS_{V-VI}
M052X/SMD	38.6	8.2	34.4	51.9
B3LYP/CPCM	34.4	12.2	27.6	43.2
SCSRIMP2/COSMO	25.1	4.9	46.7	48.9

The outcomes of the investigation performed at the MP2 level of theory (figure S2) show that the last step of the whole process continues to be rate determining, whereas the pathway (a) is evidently indicated as the preferred one, due the very high calculated value of the height of the energy barrier, 46.7 kcal/mol, for the second step of the (b) pathway. Thus, the discrepancies among

the outcomes of the computations performed at different levels of theory do not allow to give an unambiguous indication of the most likely mechanism.

[π2 + π2] cycloaddition pathway: formation of benzaldehydes, via a dioxetane intermediate

According to the results reported in literature about the oxidation of *cis*-resveratrol, the pathway via singlet oxygen addition to the exocyclic double bond to furnish the dioxetane is more favorable both kinetically and thermodynamically than the formation of the other product, diphenylacetylene derivative taken into account by the authors.[17] This suggests us that the quenching of $^1O_2$ by resveratrol and its oligomers should follow a pathway different from that hypothesized by Jiang et al.[15]

In Figures 4 and 5 are reported the energy profile and the optimized geometries, respectively of all the stationary points intercepted along the [π2 + π2] cycloaddition pathway at M052X level,. In analogy to the alternative investigated pathway, only the M052X optimized structures are shown in Figure 5 and commented here, while the B3LYP ones are included in the SI.

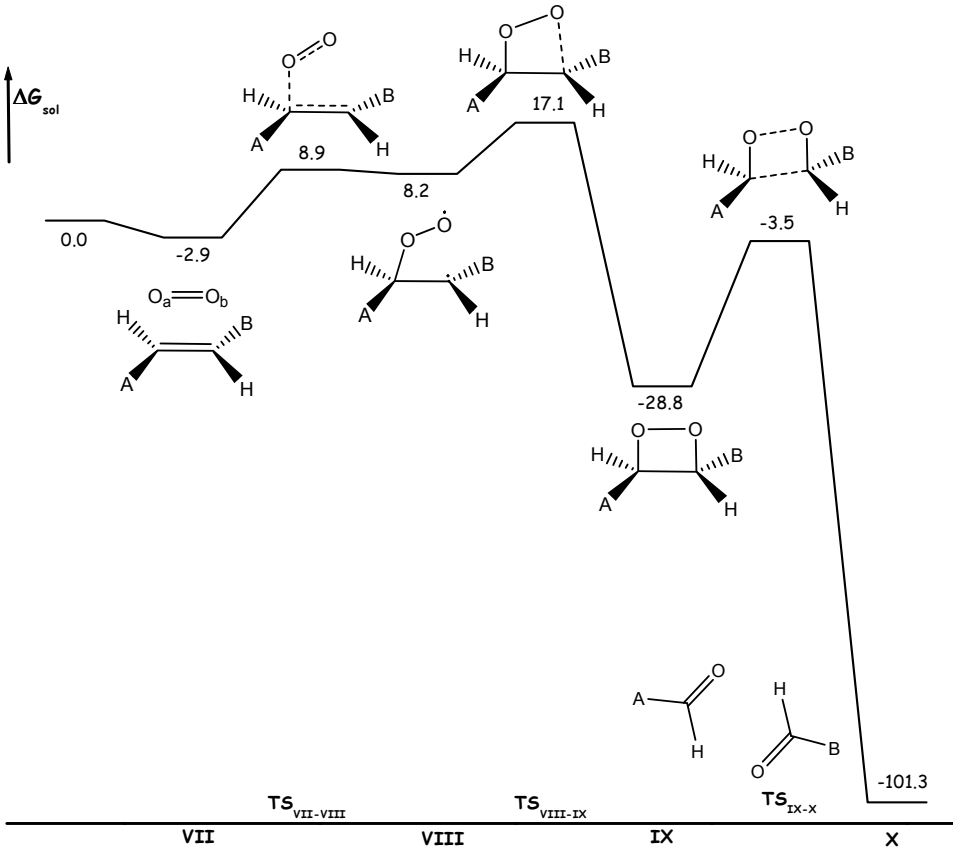

Figure 4. M052X free energy profile for the [π2 + π2] cycloaddition pathway.

As can be seen in Figure 4, the preliminary adduct **VII**, in which the $^1O_2$ weakly interacts with the exocyclic double bond (C1=C2) of *trans*-resveratrol, lies 2.9 kcal/mol below the reference energy of reactants. In the optimized structure, the O_b-O_a-C1 angle is 113.1° and the O_a-O_b-C1-C2 dihedral angle was found to be 66.0°. The O-O distance remains almost the same than that of the $^1O_2$ isolated molecule (1.217 Å *vs* 1.215 Å), confirming a very weak interaction between reactants. The reaction starts with the attack of $^1O_2$ to the C1 atom of the exocyclic double bond (see Scheme 2) to form the intermediate **VIII** through the **TS$_{VII-VIII}$**, which requires 11.8 kcal/mol to be surmounted. In the transition state **TS$_{VII-VIII}$**, the O_a atom comes close to the C1 one at a distance of 1.953 Å, while the O_a-O_b bond lengthens up to 1.266 Å. The approach of the O_a atom to the C1 one leads to a change in the dihedral angle O_b-O_a-C1-C2, which now is 78.8°, with respect to the previous minimum. The formed diradical intermediate **VIII** is destabilized by 11.1 kcal/mol than

the previous minimum. In the intermediate **VIII**, the O_a-C1 bond is formed, being 1.488 Å the distance that separates the two atoms, while the O_a-O_b bond is about 0.1 Å longer than the distance measured in the transition state leading to its formation.

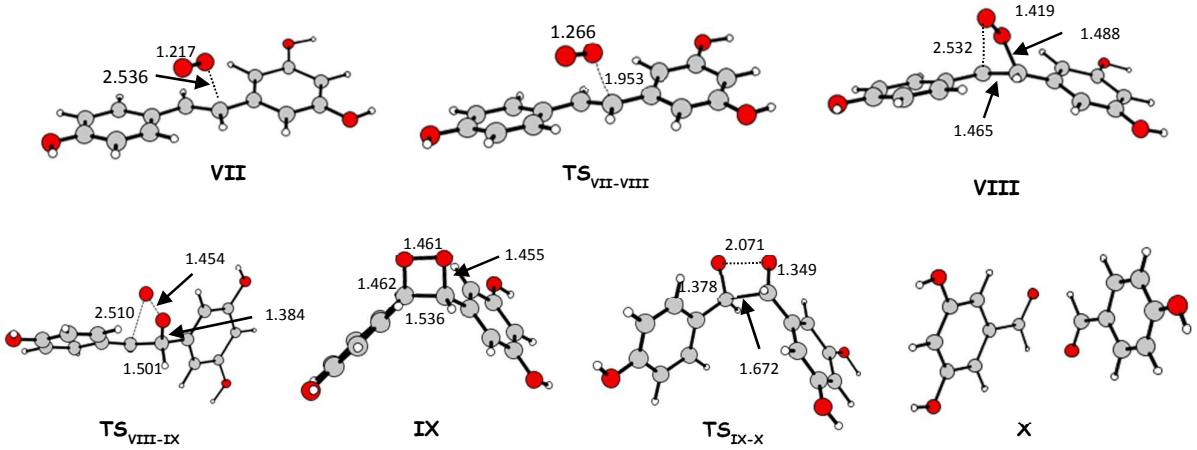

Figure 5. Optimized structures of all the intermediates and transition states intercepted along the [π2 +π2] cycloaddition pathway.

The subsequent transition state (**$TS_{VIII-IX}$**) intercepted along this path allows the formation of a dioxetane intermediate, which requires 8.9 kcal/mol to occur. In the transition state, **$TS_{VIII-IX}$**, the dihedral angle O_b-O_a-C1-C2 becomes -41.6°, while the O_b atom lies at 2.510 Å from C2. The O_a-O_b bond is significantly longer than in the previous minimum (1.454 Å *vs* 1.419 Å), as well as the C1-C2 distance that now is 1.501 Å. The formed dioxetane intermediate **IX** , lying 28.8 kcal/mol below the reactants' reference energy, is characterized by a 4-membered ring, which deviates from planarity by only 13.0°. To form the ring, all the involved bonds become longer than in the previous transition state, except the just formed O_b-C2 bond, which now is 1.462 Å. The reaction proceeds with the formation of the final products, through the transition state, **TS_{IX-X}**, which requires 25.3 kcal/mol to be formed. In the **TS_{IX-X}** , both O_a-O_b and C1-C2 bonds result almost completely broken, being 2.071 and 1.672 Å, respectively. The products, 3,5-dihydroxyl benzaldehyde and 4-hydroxyl benzaldehyde, are thus formed with an energy gain of 98.6 kcal/mol. Comparison with the

outcomes of the theoretical exploration for the *cis*-resveratrol isomer analogous pathway[17] for the dioxetane formation shows that the *trans* isomer is more active in $^1O_2$ quenching.

In analogy with mechanism 1, additional calculations were carried out employing the hybrid B3LYP exchange-correlation functional and the MP2 level of theory. The outcomes of such calculations are collected in Table 2.

Table 2. Activation barriers (in kcal/mol) corresponding to the products formation computed at different levels of theory.

	$\Delta G^{\ddagger}$
M052X/SMD	25.3
B3LYP/CPCM	18.8
SCSRIMP2/COSMO	23.8

Conclusions

In this work, we have carried out a systematic study on the reactivity of *trans*-resveratrol toward molecular oxygen in its metastable state $^1\Delta_g$ in acetone simulated media using both density functional quantum chemistry and second-order Möller-Plesset perturbation theory (MP2). Two possible mechanisms were investigated. The first is that proposed on the basis of the assumption that resveratrol and its oligomers quench $^1O_2$ via a mechanism similar to that of phenol. Two viable alternative pathways that could lead to the resveratrol quinone formation were explored. One in which the singlet molecular oxygen is the only reactant involved in the formation of the final product and one in which a water molecule assists the quenching mechanism. The second mechanism was explored according to the hypothesis that the $^1O_2$ could be quenched by the exocyclic double bond connecting the two functionality of resveratrol, the resorcinol and the phenol rings, leading to benzaldeydes formation.

The reaction between trans-resveratrol and $^1O_2$ according to the former mechanism, involving the formation of an endoperoxide intermediate was fully explored. Whether a water molecule participates in the reaction or not, the step that controls the reaction rate remains the last one, that is the release of a water molecule from the hydroperoxide intermediate to form the resveratrol quinone product. Since this step involves the H-abstraction from a C atom of the resorcinol ring, the energy barrier is obviously high. Due to the discrepancies between the employed theoretical approaches, it is not possible to clearly indicate which is the most probable pathway. On the basis of the outcomes of our quantum chemical analysis, contrary to the conclusion that can be drawn on the basis of PM3 semi-empirical molecular orbital calculations, appears to be unlikely that resveratrol and its oligomers quench $^1O_2$ via a mechanism similar to that of phenol. Our calculations suggest, instead, that the [π2 + π2] cycloaddition pathway should be the preferred one, since it requires the overcoming of an energy barrier of 25.3 kcal/mol, which is significantly lower than that calculated for the 1,4-cycloaddition mechanism.

Acknowledgment. The University of Calabria, the Food Science and Engineering Interdepartmental Center of University of Calabria and L.I.P.A.C., Calabrian Laboratory of Food Process Engineering (Regione Calabria APQ - Ricerca Scientifica e Innovazione Tecnologica I atto integrativo, Azione 2 laboratori pubblici di ricerca mission oriented interfiliera, and Azione 3 sostegno alla domanda di innovazione nel settore agroalimentare) and the PON R&C (Programma Operativo Nazionale Ricerca e Competitività 2007–2013) project PON01_00293 “Spread Bio Oil” are gratefully acknowledged.

Electronic Supplementary Information (ESI) available: Energy profile computed for the 1,4-cycloaddition mechanism by employing B3LYP exchange and correlation functional, within the SMD approach. Total free energies are reported in kcal/mol. Energy profile computed for the 1,4-cycloaddition mechanism performing single point calculation at the SCS-RI-MP2 level, within the

COSMO approach. Total free energies are reported in kcal/mol. Fully optimized structures of stationary points intercepted along the 1,4-cycloaddition mechanism by employing B3LYP exchange and correlation functional, within the CPCM approach. Energy profile computed for the [π2 + π2] cycloaddition mechanism by employing B3LYP exchange and correlation functional, within the CPCM approach. Total free energies are reported in kcal/mol. Energy profile computed for the [π2 + π2] cycloaddition mechanism performing single point calculation at the SCS-RI-MP2 level, within the COSMO approach. Fully optimized structures of stationary points intercepted along the [π2 + π2] cycloaddition mechanism by employing B3LYP exchange and correlation functional, within the CPCM approach. See DOI: 10.1039/b000000x/

References

1. a) P. Langcake, R. Pryce, *J. Physiol. Plant. Pathol.,* 1976, **9**, 77-86; L. Fremont, *Life Sci.* 2000, **66**, 663-673.
2. a) P. Langcake, R. J. Pryce, *Phytochemistry,* 1977, **16**, 1193-1196; b) G. J. Soleas, E. P. Diamandis, D. M. Goldberg, *Clin. Biochem.,* 1997, **30**, 91-113; c) E. H. Siemann, L. L. Creasy, *Amer. J. Enol. Vitic.,* 1992, **43**, 49-52.
3. J.-P. Basly, F. Marre-Fournier, J.-C. Le Bail, G. Habrioux, A. J. Chulia, *Life Sci.,* 2000, **66**, 769-777.
4. a) M. F. Wang, J. G. Li, M. Rangarajan, Y. Shao, E. J. Lavoie, T. C. Huang, C. T. Ho, *J. Agric. Food Chem.,* 1998, **46**, 4869-4873; b) O. Brede, S. Stojanovics, H. Sprinz, *Free Radic. Res.,* 2002, **36**, 76-77; P. Brito, L. M. Almeida, T. C. Dinis, *Free Radic. Res.,* 2002, **36**, 621-631; c) D. Pietraforte, L. Turco, E. Azzini, M. Minetti, *Biochim. Biophys. Acta,* 2002, **1583**, 176-184; d) B. Tadolini, C. Juliano, L. Piu, F. Franconi, L. Cabrini, *Free Radic. Res.,* 2000, **33**, 105-114; e) L. M. Szewczuk, L. Forti, L. A. Stivala, T. M. Penning, *J. Biol. Chem.*, 2000, **279**, 22727-22737; f) L. Belguendoz, L. Fremont, A. Linard, *Biochem. Pharm.*, 1997, **33**, 1347-1355; g) L. Fremont, L. Belguendouz, S. Delpal, *Life Sci.*, 1999, **64**, 2511-2521; h) M. Murias, N. Handler, T. Erker, K. Pleban, G. Ecker, P. Saiko, T. Szekeres, W. Jäger, *Bioorg. Med. Chem.*, 2004, **12**, 5571-5578; i) R. A. Baxter, *J. Cosmet. Dermatol.* 2008 Mar, **7**(1), 2-7.

5. a) J. K. Chen, S. E. Chow, *Chang Gung Med. J.* 2005, **28**, 369–377; b) I. Rahman, S. K. Biswas, P. A. Kirkham, *Biochem Pharmacol,* 2006, **72**, 1439–1452.
6. a) J. L. Mark, *Science,* 1987, **235**, 529–531; b) G.B. Bulkley, *Surgery*, 1983, **94**, 407–411.
7. B. Halliwell, R. Aeschbach, J. Löliger, O. I. Aruoma, *Fd Chem Toxic,* 1995, **33**, 601–617.
8. C. Iuga, J. R. Alvarez-Idaboy, N. Russo, *J. Org. Chem.,* 2012, **77**, 3868−3877.
9. K. Briviba, L. O. Klotz, H. Sies, *Biol. Chem.*, 1997, **378**, 1259-1265.
10. C. Kiryu, M. Makiuchi, J. Miyazaki, T. Fujinaga, K. Kakinuma, *FEBS Lett*., 1999, **443**, 154–158.
11. J. Baier, T. Maisch, M. Maier, E. Engel, M. Landthaler, W. Bäumler, *Biophys. J.*, 2006, **91**, 1452–1459.
12. E. Cadenas, H. Sies, *Methods Enzymol,* 1984, **105**, 221–231.
13. M. Y. Li, C. S. Cline, E.B. Koker, H. H. Carmichael, C. F. Chignell, P. Bilski, *Photochem Photobiol.*, 2001 Dec, **74**(6), 760-764.
14. A. Ouchi, K. Aizawa, Y. Iwasali, T. Inakuma, J. Terao, S.-I. Nagaoka, K. Mukai, *J. Agric. Food Chem.*, 2010, **58**, 9967–9978.
15. L.-Y. Jiang, S. He, K.-Z. Jiang, C.-R. Sun, Y.-J. Pan, *J. Agric. Food Chem.*, 2010, **58**, 9020–9027.
16. J. J. Chen, S. He, H. Mao, C. R. Sun, Y. J. Pan, *Rapid Commun. Mass Spectrom.*, 2009, **23**, 737–744.
17. R. Á. Rodríguez, I. R. Lahoz, O. N. Faza, M. M. Cid, C. Silva Lopez, *Org. Biomol. Chem.*, 2012, **10**, 9175-9182.
18. Becke, A. D., *J. Chem. Phys.,* 1993, **98**, 5648-5652.
19. P. J. Stephens, F. J. Devlin, C. F. Chabalowski, M. J. Frisch, *J. Phys. Chem.,* 1994, **98**, 11623-11627.
20. Y. Zhao, N. E. Schultz, D. G. Truhlar, *J. Chem. Theory and Comput.*, 2006, **2**, 364-382.
21. Y. Zhao, D. G. Truhlar, *J. Phys. Chem. A*, 2008, **112**, 1095-1099.
22. M. Cossi, N. Rega, G. Scalmani, V. Barone, *J. Comput. Chem.*, 2003, **24**, 669-681.
23. A. V. Marenich, C. J.Cramer, D. G. Truhlar, *J. Phys. Chem. B*, 2009, **113**, 6378–6396.
24. a) K. Fukui, *J. Phys. Chem.*, 1970, **74**, 4161-4163; b) C. Gonzalez, H. B. Schlegel, *J. Chem. Phys.*, 1989, **90**, 2154-2161.
25. C. Möller, M. S. Plesset, *Phys. Rev.*, 1934, **46**, 618-622.

26. R. Ahlrichs, M. Bär, M. Häser, H. Horn, C. Kölmel, *Chem. Phys. Lett*., 1989, **162**, 165–169.

27. S. Grimme, *J. Chem. Phys.*, 2003, **118**, 9095-9102.

28. A. A. Ovchinnicov, J. K. Labanowski, *Phys. Rev. A*, 1996, **53**, 3946-3952.